Southampton, United Kingdom; [8]*Farjo Hair Institute, London, United Kingdom;* [9]*Department of Dermatology and Venereology of NHS, Andreas Syggros Hospital of Skin and Venereal Diseases, Athens, Greece;* [10]*Trichology Unit, Dermatology Department, Ramon Y Cajal Hospital, IRYCIS, University of Alcala, Madrid, Spain;* [11]*Servicio de Dermatología, Hospital del Mar-Parc de Salut Mar, Barcelona, Spain;* [12]*Barcelona Institute for Global Health (ISGlobal), Barcelona, Spain;* [13]*Dermatology Unit, IRCCS Azienda Ospedaliero-Universitaria di Bologna, Bologna, Italy;* [14]*Department of Medical and Surgical Sciences, Alma Mater Studiorum - University of Bologna, Bologna, Italy;* [15]*Harvard Medical School and Lahey Hospital and Medical Center, Boston, Massachusetts;* [16]*Department of Dermatology, Venereology and Allergology, Charité-Universitätsmedizin Berlin, Berlin, Germany;* [17]*Department of Dermatology, Venerology, Allergology and Phlebology, Johannes Wesling Medical Centre, University Hospital of the Ruhr University of Bochum, Minden, Germany; and* [18]*Department of Medical and Molecular Genetics, King's College London, London, United Kingdom*

[19]*These authors contributed equally to this work.*

[*]*Corresponding author. e-mail: christos.tziotzios@kcl.ac.uk*

SUPPLEMENTARY MATERIAL

Supplementary material is linked to the online version of the paper at www.jidonline.org, and at https://doi.org/10.1016/j.jid.2023.04.022.

REFERENCES

Harries MJ, Meyer K, Chaudhry I, E Kloepper J, Poblet E, Griffiths CEM, et al. Lichen planopilaris is characterized by immune privilege collapse of the hair follicle's epithelial stem cell niche. J Pathol 2013;231:236–47.

Kanti V, Constantinou A, Reygagne P, Vogt A, Kottner J, Blume-Peytavi U. Frontal fibrosing alopecia: demographic and clinical characteristics of 490 cases. J Eur Acad Dermatol Venereol 2019;33:1976–83.

Kurzawski M, Dziedziejko V, Post M, Wójcicki M, Urasińska E, Miętkiewski J, et al. Expression of genes involved in xenobiotic metabolism and transport in end-stage liver disease: up-regulation of ABCC4 and CYP1B1. Pharmacol Rep 2012;64:927–39.

Lobato-Berezo A, Iglesias-Sancho M, Rodríguez-Lomba E, Mir-Bonafé JF, Velasco-Tamariz V, Porriño-Bustamante ML, et al. Frontal fibrosing alopecia in men: a multicenter study of 39 patients. J Am Acad Dermatol 2022;86:481–4.

Rayinda T, McSweeney SM, Dand N, Fenton DA, McGrath JA, Tziotzios C. Clinical characteristics of male frontal fibrosing alopecia: a single-centre case series from London. UK. Br J Dermatol 2022;186:195–7.

Shah BR, Xu W, Mraz J. Cytochrome P450 1B1: role in health and disease and effect of nutrition on its expression. RSC Adv 2019;9:21050–62.

Shimada T, Watanabe J, Kawajiri K, Sutter TR, Guengerich FP, Gillam EM, et al. Catalytic properties of polymorphic human cytochrome P450 1B1 variants. Carcinogenesis 1999;20:1607–13.

Tziotzios C, Petridis C, Dand N, Ainali C, Saklatvala JR, Pullabhatla V, et al. Genome-wide association study in frontal fibrosing alopecia identifies four susceptibility loci including HLA-B*07:02. Nat Commun 2019;10:1150.

Vañó-Galván S, Molina-Ruiz AM, Serrano-Falcón C, Arias-Santiago S, Rodrigues-Barata AR, Garnacho-Saucedo G, et al. Frontal fibrosing alopecia: a multicenter review of 355 patients. J Am Acad Dermatol 2014;70:670–8.

Antigen Protease Activity with a Detergent Induces Severe Skin Inflammation with Itch and Robust T Helper 17/T Helper 22 Differentiation in Mice

Journal of Investigative Dermatology (2023) **143,** 2314–2318; doi:10.1016/j.jid.2023.03.1685

TO THE EDITOR

We previously reported some models of epicutaneous (e.c.) sensitization of C57-BL/6 mice with the model protease antigen, papain (Iida et al., 2014; Ochi et al., 2017; Shimura et al., 2016), which is an occupational allergen that belongs to the same cysteine protease family as the house dust mite major protease allergens (Takai and Ikeda, 2011) and the staphylococcal cysteine proteases (Williams et al., 2020). However, our previous models did not show the promotion of chronic itch–induced scratching behaviors 1 day after the last e.c. administration of papain. Therefore, in this study, we established and characterized a model of sensitization with papain through detergent-treated skin, which showed severely exacerbated skin inflammation with itch, the induction of antigen-specific IgE, and the differentiation of a number of T helper (Th) subsets. We also identified the responses that were dependent on the protease activity of papain. All animal experiments were approved by the Committee on Animal Experiments of Juntendo University (Tokyo, Japan).

SDS is a detergent present in shampoo and body soap that is used on a daily basis (Masutani et al., 2022). We modified our previous model with treatment with 4% SDS just before the application of papain (Ochi et al., 2017) and established the present model with a daily 10% SDS treatment of a wide ear skin area with increasing volumes of SDS and papain. The treatment with SDS plus papain induced an earlier increase in ear thickness than treatment with SDS plus vehicle, and papain-specific IgE was produced in a dose-dependent manner (Supplementary Figure S1). The treatment with SDS plus papain (10 mg/ml papain) induced more severe ear swelling with skin inflammation, greater transepidermal water loss, and more frequent hind-paw scratching behavior than treatment with SDS plus vehicle. Histology showed epidermal hyperplasia and swelling of the dermis with the infiltration of neutrophils and eosinophils in mice treated with SDS plus

Abbreviations: DLN, draining lymph node; e.c., epicutaneous; OVA, ovalbumin; Th, T helper

Accepted manuscript published online 23 May 2023; corrected proof published online 22 July 2023

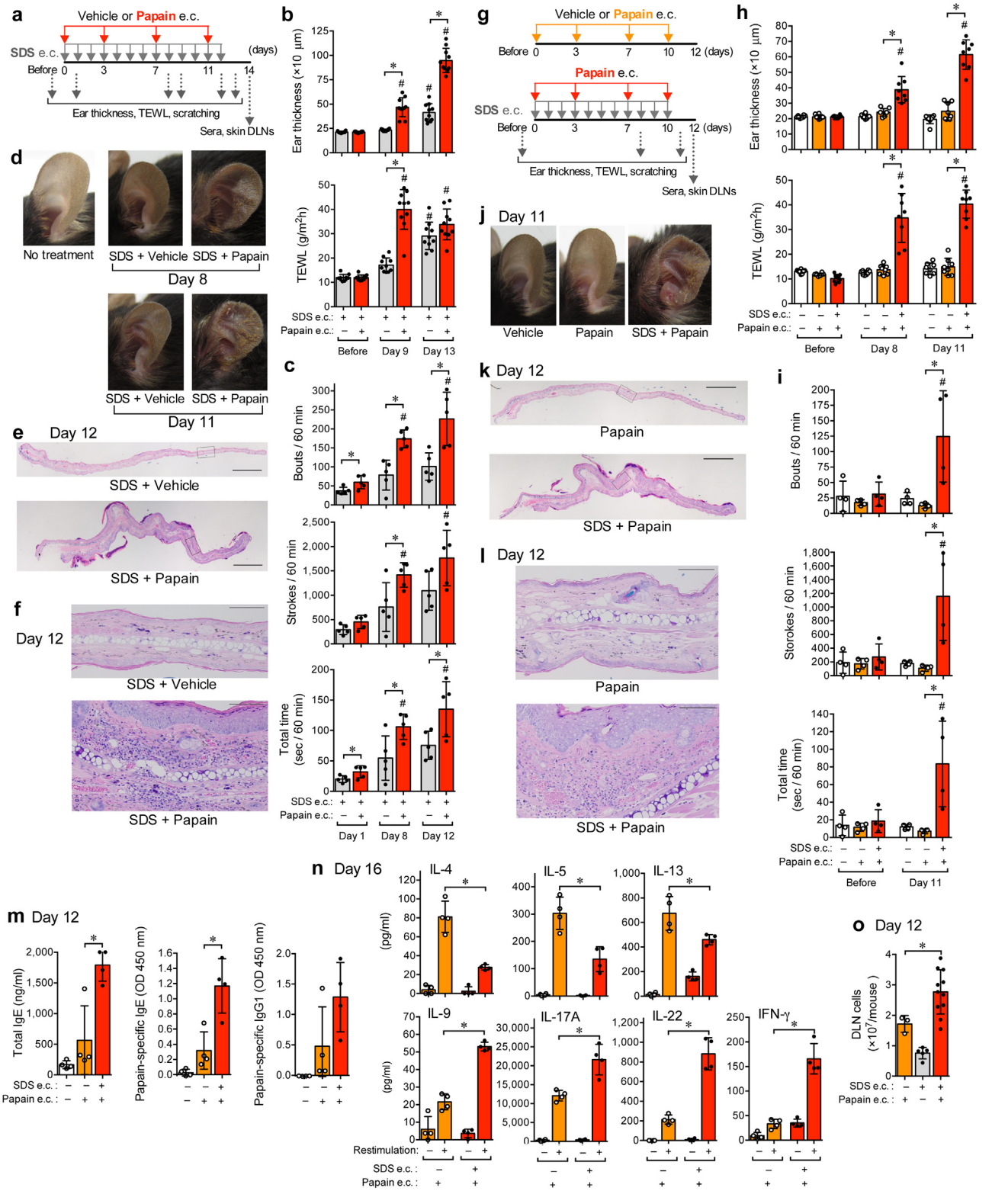

Figure 1. Epicutaneous administration of papain exacerbated SDS-induced itch-associated dermatitis with the production of serum papain−specific IgE and differentiation of a number of Th subsets. Vehicle or papain (10 mg/ml) was applied to the ear skin with or without the SDS treatment. (**a**, **g**) Timelines for (**a**) **b**−**f** and (**g**) **h**−**o**. (**b, h**) Ear thickness and TEWL (n = 10 in **b**, n = 8 in **h**). (**c, i**) Scratching behaviors (n = 5 in **c**, n = 4 in **i**). (**d, j**) Appearance. (**e, f, k, l**) Histology. Bars = 1 mm (for **e** and **k**) and 0.1 mm (for **f** and **l**). (**m**) Serum antibodies (n = 4). (**n**) Cytokine responses in skin DLN cells restimulated with E64-papain for 4 days (4 wells). (**o**) Total DLN cell numbers recovered. Data indicate means ± SD and are representative of two or more independent experiments, except for data in panel **o**, in which each of the data points represents the averaged value in each of the independent experiments (n = 3, 5, and 11, respectively). *$P < 0.05$ versus SDS e.c. treatment + vehicle e.c. treatment by the *t*-test (for **b** and **c**) or versus papain e.c. treatment (for **h, i, and m**−**o**) and #$P < 0.05$ versus measurements before the start of the experiments except for **c** (vs. day 1) by ANOVA. DLN, draining lymph node; e.c., epicutaneous; min, minute; TEWL, transepidermal water loss; Th, T helper.

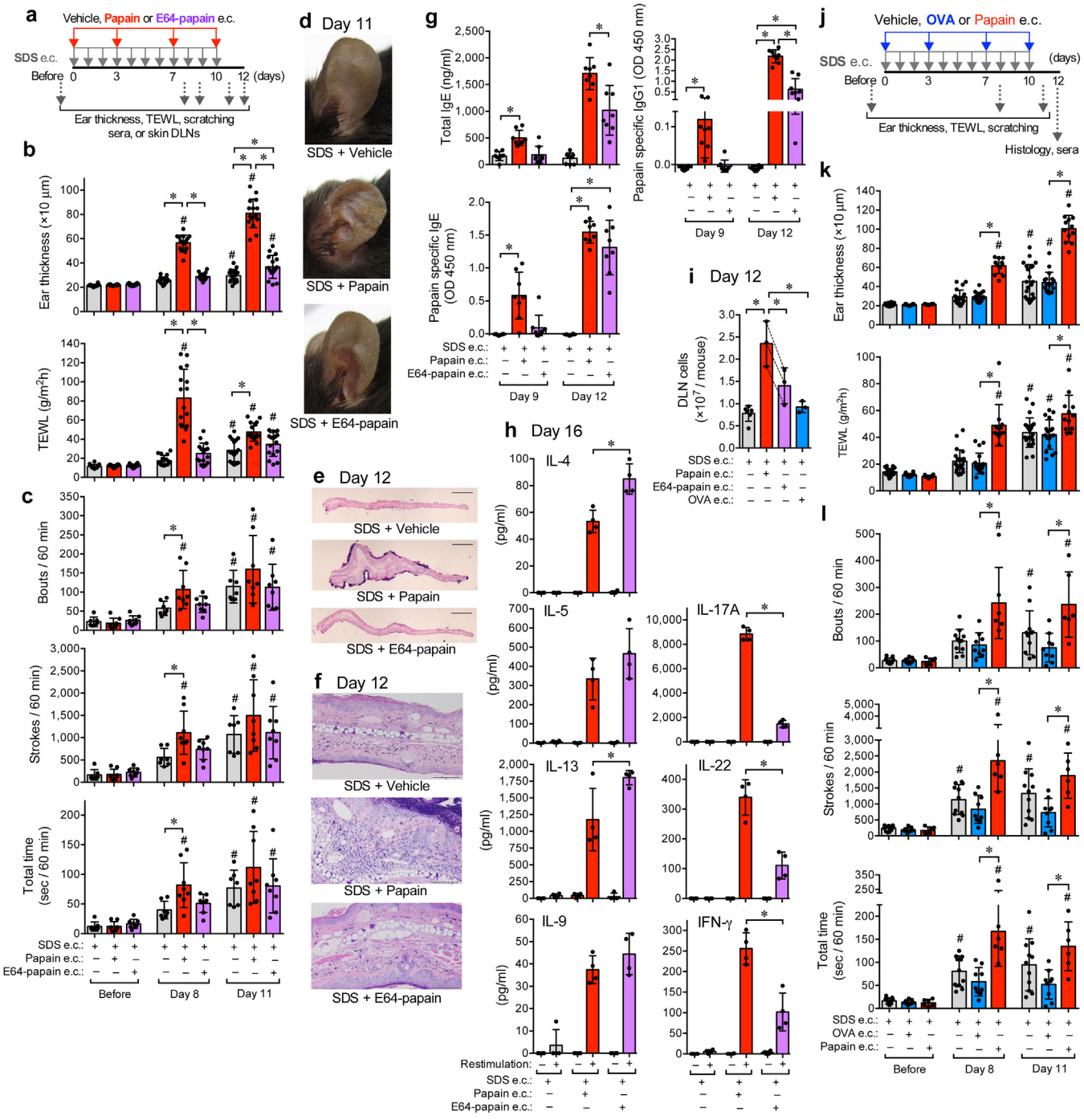

Figure 2. Papain protease activity in SDS-treated skin was essential for the exacerbated symptoms of dermatitis, rapid IgE elevations, and the differentiation of Th17/Th22/Th1 but not of Th2/Th9. Vehicle, papain, protease inhibitor–treated papain (E64-papain), or OVA (10 mg/ml) were applied to SDS-treated ear skin. (**a, j**) Timelines for (**a**) **b–i** and (**j**) **k and l**. (**b, k**) Ear thickness and TEWL (n = 16 in **b**; n = 22, 18, and 12 for the three mouse groups, respectively, in **k**). (**c, l**) Scratching behaviors (n = 8 in **c**; n = 11, 9, and 6 in **l**). (**d**) Appearance. (**e, f**) Histology. Bars = 1 mm (in **e**) and 0.1 mm (in **f**). (**g**) Serum antibodies (n = 8). (**h**) Cytokine responses in skin DLN cells restimulated with E64-papain for 4 days (4 wells). (**i**) Total cell numbers of DLN cells recovered. Data indicate means ± SD and are representative of two or more independent experiments, except for data in panel **i**, in which each of the data points represents the averaged value in each of the independent experiments (n = 6, 3, 3, and 3, respectively), and the values for the papain e.c. treated and E64-papain e.c. treated groups obtained in the same independent experiments are linked with broken lines. *$P < 0.05$ among the mouse groups and #$P < 0.05$ versus measurements before the start of the experiments by ANOVA for all data groups, except for those in **c** (the three mouse groups). DLN, draining lymph node; e.c., epicutaneously; min, minute; OVA, ovalbumin; TEWL, transepidermal water loss; Th, T helper.

papain (Figure 1a–f). It also elevated serum total IgE levels and promoted the production of papain-specific IgE and IgG1 as well as the Th2 (IL-4, IL-5, and IL-13), Th9 (IL-9), Th17/Th22 (IL-17A and IL-22), and Th1 (IFN-γ) cytokines in antigen-restimulated skin draining lymph node (DLN) cells (Supplementary Figure S2a and b).

In contrast to the responses induced by the e.c. administration of papain through SDS-treated skin, responses induced by the administration through intact skin did not cause ear swelling with skin inflammation, transepidermal water loss increase, or scratching behaviors (Figure 2g–l) but induced weaker serum total and papain-specific IgE responses (Figure 2m). The production of Th cytokines was higher for Th2 cytokines and lower for Th9, Th17/Th22, and Th1 cytokines in antigen-restimulated skin DLN cells from mice treated with papain alone than in those from mice treated with SDS plus papain. Because DLN cell numbers were higher in mice treated with SDS plus papain than in those treated with papain alone, the total production capacity of DLN for Th cytokines was considered to be greater for Th17/Th22, Th1, and Th9 cytokines in mice treated with SDS plus papain than in those treated with papain alone and was similar for Th2 cytokines with and without the SDS treatment (Figure 2n and o). On the basis of differences in serum dilution factors and the use of signal enhancer solutions in ELISA, papain-specific IgG2b and IgG2c levels were markedly lower than papain-specific IgG1 levels (Supplementary Figure S2c).

We assessed the capacity of E64-papain (a covalent complex between cysteine protease inhibitor E-64 and papain), which retains the tertiary structure and T/B-cell epitopes of papain but lacks its protease activity (Nishioka et al., 2018) to induce responses. The treatment with SDS plus E64-papain did not exacerbate or only slightly exacerbated skin inflammation, barrier dysfunction, and scratching behaviors (Figure 2a–f and Supplementary Figure S3a and b). Furthermore, the induction of papain-specific IgE and IgG1 was slower (Figure 2g and Supplementary Figure S3c), and skin DLN cell production was similar or slightly higher for Th2 and Th9 cytokines and less for Th17/Th22 and Th1 cytokines in mice treated with SDS plus E64-papain than in those treated with SDS plus papain. Because DLN cell numbers were lower in mice treated with SDS plus E64-papain than in those treated with SDS plus papain, the total production capacity of DLN for Th17/Th22 and Th1 cytokines but not for Th2 and Th9 cytokines was considered to critically depend on papain protease activity in SDS-treated skin (Figure 2h and i and Supplementary Figure S3d and e). A recent report also described that IL-17A but not IL-4 production in restimulated DLN cells was dependent on the protease activity of papain epicutaneously applied through back skin for a longer period in HOS:TR-1 hairless mice (Ogasawara et al., 2022).

The treatment with SDS plus ovalbumin (OVA), a nonprotease antigen frequently used as an experimental model antigen, did not enhance ear swelling with skin inflammation, barrier dysfunction, or scratching behaviors, and serum OVA-specific antibody responses were not detected (Figure 2j–l and Supplementary Figure S4). Therefore, the protease-independent property of E64-papain to promote Th2 sensitization was superior to that of OVA when administered on SDS-treated skin. Although the reasons for the higher immunogenicity of E64-papain than that of OVA are unknown, it may be attributed to their different molecular sizes, possible differences in complex structures with SDS, and/or unknown properties. SDS-inducible barrier dysfunction may exhibit a preference for the penetration of 23-kDa E64-papain over 45-kDa OVA. A model with a longer period of OVA e.c. application through shaved and tape-stripped back skin in BALB/c mice has been used in many studies.

In conclusion, in this study, we showed that papain protease activity and SDS-treated skin synergistically promoted skin inflammation associated with barrier dysfunction and itch and various types of antigen-specific adaptive immunity, features found in any one of the subtypes of atopic dermatitis (Czarnowicki et al., 2019). We found that the protease activity of papain in SDS-treated skin was essential for exacerbating the symptoms of dermatitis, Th17/Th22 and Th1 differentiation, and the accelerated induction of IgE but was dispensable for Th2 and Th9 differentiation. In addition, the capacities of E64-papain and OVA to induce adaptive immune responses differed. Environmental proteases damage barrier tissues to disrupt barrier function (Hirasawa et al., 2010; Nakamura et al., 2006; Stremnitzer et al., 2015), release or produce mediators, and possess abilities that directly or indirectly stimulate various types of cells (Halim et al., 2014; Kamijo et al., 2013; Perner et al., 2020; Takai and Ikeda, 2011). The present model may be a useful tool for investigations on crosstalk or vicious cycles among skin barrier damage, innate and adaptive immunity, and the sensory nervous system in e.c. sensitization and itch-associated skin inflammation induced by stimulation with environmental protease antigens on detergent-treated skin, thereby providing insights into protease-specific responses.

Data availability statement

There are no large datasets to deposit.

ORCIDs

Tomoko Yoshimura: http://orcid.org/0000-0003-0942-155X
Seiji Kamijo: http://orcid.org/0000-0002-7199-0473
Saori Ichikawa: http://orcid.org/0000-0002-8862-439X
Toru Kimitsu: http://orcid.org/0000-0001-7354-1164
Yurie Masutani: http://orcid.org/0000-0003-0007-4811
Saya Shimizu: http://orcid.org/0000-0003-2869-6524
Keiko Takada: http://orcid.org/0000-0001-5501-9751
Takasuke Ogawa: http://orcid.org/0000-0001-7103-3254
Mitsutoshi Tominaga: http://orcid.org/0000-0002-1254-1803
Kenji Takamori: http://orcid.org/0000-0002-0644-0504
Hideoki Ogawa: http://orcid.org/0000-0003-4268-8790
Ko Okumura: http://orcid.org/0000-0003-3238-6422
Shigaku Ikeda: http://orcid.org/0000-0002-7520-0707
Toshiro Takai: http://orcid.org/0000-0001-8363-035

CONFLICT OF INTEREST

The authors state no conflict of interest.

ACKNOWLEDGMENTS

We thank Yuji Takeda (Takeda LabDesign) for technical advice for the MicroAct/ANIMA analysis; Misaki Mochida, Yoko Morita, Saki Kazaana, Mayuna Imai, Yuri Otsuka (Japan Women's University, Tokyo, Japan); Suchiva Punyada, Natsuko Maruyama, Mutsuko Hara, and Taito Yamanashi for their technical assistance; Eriko Komiya for technical advice for the SCLABA analysis; Toyoko Hidano, Fumio Kanai, and Norihiro Tada (Juntendo University Graduate School of Medicine, Tokyo, Japan) for animal care; the staff of the Laboratory of Morphology and Image Analysis of Juntendo University Graduate School of Medicine for specimen preparation for histology; and Michiyo Matsumoto and Emi Yamaguchi for their secretarial assistance. This study was supported by the Japan Society for the Promotion of Science KAKENHI, Japan (grant numbers JP22K08529, JP18K08417, and JP17K10007).

AUTHOR CONTRIBUTIONS

Conceptualization: TT, TY; Data Curation: TY, TT, SK, Saori Ichikawa, TK, YM, SS, Keiko Takada, Formal Analysis: TY, TT, SK, TK, YM, SS, Saori

Ichikawa, Keiko Takada; Funding Acquisition: TT, SK, KO, Shigaku Ikeda; Investigation: TY, TT, SK, Saori Ichikawa, TK, YM, SS, TO, Keiko Takada; Methodology: TY, TT, SK, TK, YM, SS, TO, Saori Ichikawa, Keiko Takada; Project Administration: TT, TY, SK, KO, Shigaku Ikeda, HO; Resources: TM, Kenji Takamori; Supervision: TT, KO, Shigaku Ikeda; Visualization: TY, TT, SK; Writing - Original Draft Preparation: TY, TT; Writing - Review and Editing: TT, TY, SK, Saori Ichikawa, TK, YM, SS, Keiko Takada, TO, MT, Kenji Takamori, HO, KO, Shigaku Ikeda.

***Tomoko Yoshimura*[1,2], *Seiji Kamijo*[1], *Saori Ichikawa*[3], *Toru Kimitsu*[1,2], *Yurie Masutani*[1,2], *Saya Shimizu*[1], *Keiko Takada*[1,2], *Takasuke Ogawa*[2], *Mitsutoshi Tominaga*[4], *Kenji Takamori*[4], *Hideoki Ogawa*[2], *Ko Okumura*[1], *Shigaku Ikeda*[1,2] and *Toshiro Takai*[1,*]**

[1]*Atopy (Allergy) Research Center, Juntendo University Graduate School of Medicine, Tokyo, Japan;* [2]*Department of Dermatology and Allergology, Juntendo University Graduate School of Medicine, Tokyo, Japan;* [3]*Department of Chemical and Biological Sciences, Faculty of Science, Japan Women's University, Tokyo, Japan; and* [4]*Juntendo Itch Research Center (JIRC), Institute for Environmental and Gender-Specific Medicine, Juntendo University Graduate School of Medicine, Chiba, Japan*

[*]*Corresponding author e-mail: t-takai@juntendo.ac.jp*

SUPPLEMENTARY MATERIALS

Supplementary material is linked to the online version of the paper at www.jidonline.org and at https://doi.org/10.1016/j.jid.2023.03.1685

REFERENCES

Czarnowicki T, He H, Krueger JG, Guttman-Yassky E. Atopic dermatitis endotypes and implications for targeted therapeutics. J Allergy Clin Immunol 2019;143:1–11.

Halim TY, Steer CA, Mathä L, Gold MJ, Martinez-Gonzalez I, McNagny KM, et al. Group 2 innate lymphoid cells are critical for the initiation of adaptive T helper 2 cell-mediated allergic lung inflammation. Immunity 2014;40:425–35.

Hirasawa Y, Takai T, Nakamura T, Mitsuishi K, Gunawan H, Suto H, et al. *Staphylococcus* aureus extracellular protease causes epidermal barrier dysfunction. J Invest Dermatol 2010;130:614–7.

Iida H, Takai T, Hirasawa Y, Kamijo S, Shimura S, Ochi H, et al. Epicutaneous administration of papain induces IgE and IgG responses in a cysteine protease activity-dependent manner. Allergol Int 2014;63:219–26.

Kamijo S, Takeda H, Tokura T, Suzuki M, Inui K, Hara M, et al. IL-33-mediated innate response and adaptive immune cells contribute to maximum responses of protease allergen-induced allergic airway inflammation. J Immunol 2013;190:4489–99.

Masutani Y, Takai T, Kamijo S, Kimitsu T, Yoshimura T, Ichikawa S, et al. Skin treatment with detergent induces dermatitis with H1-antihistamine-refractory itch and upregulates IL-4 and Th17/Th22 cytokine gene expression in C57BL/6 mice. Int Arch Allergy Immunol 2022;183:1040–9.

Nakamura T, Hirasawa Y, Takai T, Mitsuishi K, Okuda M, Kato T, et al. Reduction of skin barrier function by proteolytic activity of a recombinant house dust mite major allergen Der f 1. J Invest Dermatol 2006;126:2719–23.

Nishioka I, Takai T, Maruyama N, Kamijo S, Suchiva P, Suzuki M, et al. Airway inflammation after epicutaneous sensitization of mice requires protease activity of low-dose allergen inhalation. J Allergy Clin Immunol 2018;141:2271–73.e7.

Ochi H, Takai T, Shimura S, Maruyama N, Nishioka I, Kamijo S, et al. Skin treatment with detergent promotes protease allergen-dependent epicutaneous sensitization in a manner different from tape stripping in mice. J Invest Dermatol 2017;137:1578–82.

Ogasawara A, Yuki T, Katagiri A, Lai YT, Takahashi Y, Basketter D, et al. Proteolytic activity accelerates the TH17/TH22 recall response to an epicutaneous protein allergen-induced TH2 response. J Immunotoxicol 2022;19:27–33.

Perner C, Flayer CH, Zhu X, Aderhold PA, Dewan ZNA, Voisin T, et al. Substance P release by sensory neurons triggers dendritic cell migration and initiates the Type-2 immune response to allergens. Immunity 2020;53:1063–1077.e7.

Shimura S, Takai T, Iida H, Maruyama N, Ochi H, Kamijo S, et al. Epicutaneous allergic sensitization by cooperation between allergen protease activity and mechanical skin barrier damage in mice. J Invest Dermatol 2016;136:1408–17.

Stremnitzer C, Manzano-Szalai K, Willensdorfer A, Starkl P, Pieper M, König P, et al. Papain degrades tight junction proteins of human keratinocytes in vitro and sensitizes C57BL/6 mice via the skin independent of its enzymatic activity or TLR4 activation. J Invest Dermatol 2015;135:1790–800.

Takai T, Ikeda S. Barrier dysfunction caused by environmental proteases in the pathogenesis of allergic diseases. Allergol Int 2011;60:25–35.

Williams MR, Cau L, Wang Y, Kaul D, Sanford JA, Zaramela LS, et al. Interplay of staphylococcal and host proteases promotes skin barrier disruption in netherton syndrome. Cell Rep 2020;30:2923–33.e7.

Reduced Skin T-Cell Receptor Diversity in Large Cell Transformed Mycosis Fungoides

Journal of Investigative Dermatology (2023) **143,** 2318–2322; doi:10.1016/j.jid.2023.03.1683

TO THE EDITOR

Mycosis fungoides (MF) begins with a proliferation of a malignant T-cell clone in the skin that may progress to involve blood, lymph nodes, and viscera in the late stages. Large cell transformed MF (LCT-MF) is an aggressive histologic subtype associated with disease progression, recurrence, and decreased survival, even in early stages (Agar et al., 2010; O'Donnell et al., 2022). In this study, we investigate the characteristics of the T-cell repertoire in the skin and blood of patients with LCT-MF.

T-cell repertoire diversity is a metric of T-cell response in both solid and hematologic malignancies and can provide insight into the underlying biological changes in aggressive subtypes (Attaf et al., 2015; Thorsson et al., 2018; Valpione et al., 2021). In addition, skin tumor clone frequency (TCF) or the frequency of the dominant malignant clone among all T cells can influence MF prognosis (de Masson et al., 2018). The characteristics of T-cell repertoire, including T-cell diversity and TCF in the blood and skin of patients with MF who undergo large cell transformation, are not known. To assess the initial T-cell repertoire changes upon early disease transformation in the blood and skin of

Abbreviations: CDR3, complementarity determining region 3; LCT-MF, large cell transformed mycosis fungoides; MF, mycosis fungoides; TCF, tumor clone frequency; TCR, T-cell receptor

Accepted manuscript published online 29 April 2023; corrected proof published online 4 October 2023

SUPPLEMENTARY MATERIALS AND METHODS

Mice

C57/BL6J female mice (Sankyo Lab Service, Ibaraki, Japan) aged 7−12 weeks were maintained in a specific pathogen-free animal facility at Juntendo University (Tokyo, Japan).

Antigens

The E64-papain (covalent complex between cysteine protease inhibitor E-64 [Peptide Institute, Osaka, Japan] and papain [Calbiochem, San Diego, CA]) was prepared as previously described (Kamijo et al., 2013). Papain, which was incubated similarly to E64-treated papain (but without the addition of E-64) and dialyzed, was prepared and used for comparisons with E64-treated papain. Ovalbumin (OVA) (grade V; Sigma-Aldrich, St. Louis, MO) was used for epicutaneous administration and ELISA.

Epicutaneous sensitization

The ear skin of mice was treated with 10% SDS in pure water every day. Two hours or more after the SDS treatment, vehicle (PBS containing 0.5% [v/v] Tween 20), papain, E64-papain, OVA, or a mixture of OVA and papain was epicutaneously administered twice per week for 2 weeks for a total of four times. Solutions were applied with a micropipette to both sides of the surface of both ears and the dorsal hairless area at the base of the ear of lightly anesthetized mice (30 μl per ear, 60 μl per mouse). Aliquots of antigen solution were stored at −80 °C and thawed just before use.

Skin inflammation and barrier dysfunction

The ear thickness of lightly anesthetized mice was measured using a dial thickness gauge (G-1A, Ozaki, Tokyo, Japan). Paraffin-embedded sections of ear specimens were stained with Giemsa. Regarding barrier dysfunction, transepidermal water loss on the dorsal side of the ear was measured using a VapoMeter (Delfin Technologies, Kuopio, Finland) in nail mode.

Scratching behaviors

Hind-paw scratching behaviors were analyzed using the MicroAct system (Neuroscience, Tokyo, Japan) according to the method described earlier (Masutani et al., 2022) with modifications. Scratching bouts, strokes, and the total time of scratching behaviors were assessed by software (ANIMA; Takeda LabDesign, Ibaraki, Japan). In the setting of parameters, the apparatus detected consecutive scratching behaviors consisting of four or more strokes to omit false-positive signals.

Antigen restimulation of draining lymph node cells

Sera and skin draining lymph node cells (cervical lymph nodes) were collected and stimulated as previously described with modifications (Ochi et al., 2017). Briefly, skin draining lymph node cells were restimulated with medium alone or E64-papain (50 μg/ml) in 96-well round-bottomed culture plates for 96 hours (5×10^5 cells/200 μl/well). We used E64-papain as the antigen for the restimulation to avoid potential protease activity−dependent effects. Draining lymph node cells from mice in each of the mouse groups were pooled and stimulated in three or four wells.

ELISA

Serum total IgE and papain- and OVA-specific antibodies were detected on plates, which were coated with 2 μg/ml anti-murine IgE mAbs, 10 μg/ml papain, or 1 mg/ml OVA as previously described (Kamijo et al., 2021; Shimura et al., 2016; Takai et al., 2005) with modifications. Total IgE was measured by sandwich ELISA. Serum dilution factors for the detection of antigen-specific IgE, IgG1, IgG2b, and IgG2c were 50; 5,000; 250; and 250, respectively. To detect antigen-specific IgG2b and IgG2c, sera and detection antibodies were diluted with solutions 1 and 2 of CanGetSignal (Toyobo, Osaka, Japan), respectively, to enhance the signals. Cytokine and chemokine concentrations were measured with ELISA kits (R&D Systems, Minneapolis, MN), except for IL-9 (BioLegend, San Diego, CA).

Statistical analysis

The student's *t*-test (two tailed), Mann−Whitney *U* test (two tailed), or a one-way ANOVA with Tukey's posthoc test were used. A value of $P < 0.05$ was considered significant.

SUPPLEMENTARY REFERENCES

Kamijo S, Hara M, Suzuki M, Nakae S, Ogawa H, Okumura K, et al. Innate IL-17A enhances IL-33-independent skin eosinophilia and IgE response on subcutaneous papain sensitization. J Invest Dermatol 2021;141:105−113.e14.

Kamijo S, Takeda H, Tokura T, Suzuki M, Inui K, Hara M, et al. IL-33-mediated innate response and adaptive immune cells contribute to maximum responses of protease allergen-induced allergic airway inflammation. J Immunol 2013;190:4489−99.

Masutani Y, Takai T, Kamijo S, Kimitsu T, Yoshimura T, Ichikawa S, et al. Skin treatment with detergent induces dermatitis with H1-antihistamine-refractory itch and upregulates IL-4 and Th17/Th22 cytokine gene expression in C57BL/6 mice. Int Arch Allergy Immunol 2022;183:1040−9.

Ochi H, Takai T, Shimura S, Maruyama N, Nishioka I, Kamijo S, et al. Skin treatment with detergent promotes protease allergen-dependent epicutaneous sensitization in a manner different from tape stripping in mice. J Invest Dermatol 2017;137:1578−82.

Shimura S, Takai T, Iida H, Maruyama N, Ochi H, Kamijo S, et al. Epicutaneous allergic sensitization by cooperation between allergen protease activity and mechanical skin barrier damage in mice. J Invest Dermatol 2016;136:1408−17.

Takai T, Kato T, Ota M, Yasueda H, Kuhara T, Okumura K, et al. Recombinant Der p 1 and der f 1 with in vitro enzymatic activity to cleave human CD23, CD25 and alpha1-antitrypsin, and in vivo IgE-eliciting activity in mice. Int Arch Allergy Immunol 2005;137:194−200.

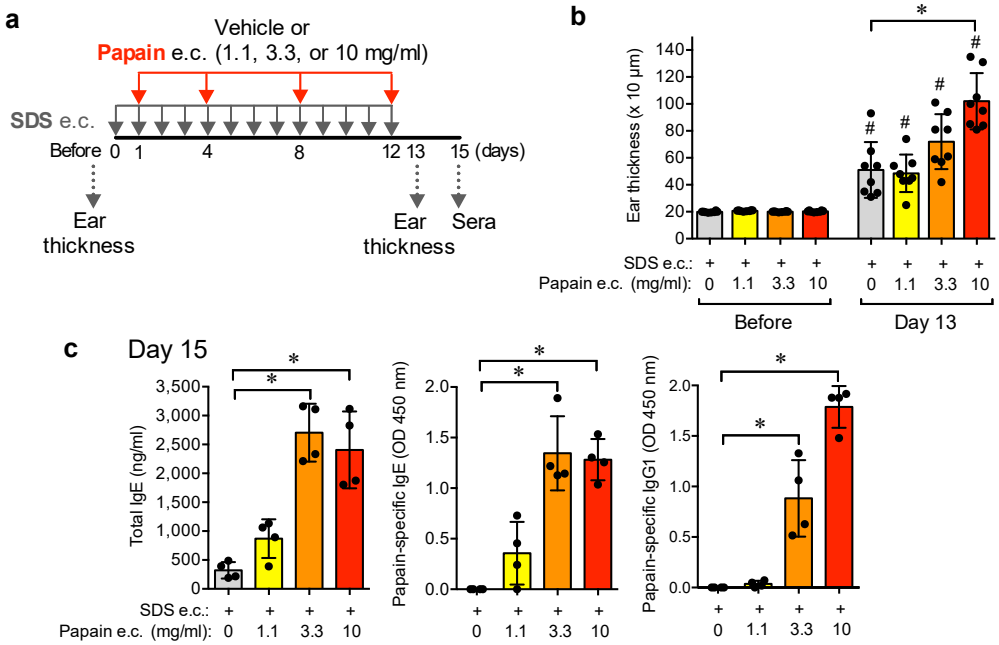

Supplementary Figure S1. Epicutaneous papain administration through SDS-treated skin induced increases in ear thickness and the production of serum papain−specific IgE in a dose-dependent manner. Vehicle or papain (1.1, 3.3, or 10 mg/ml) was applied to SDS-treated ear skin. (**a**) Timeline. (**b**) Ear thickness (n = 8). (**c**) Serum antibodies (n = 4). Data indicate means ± SD and are representative of two or more independent experiments. *$P < 0.05$ by ANOVA with Tukey's posthoc test and #$P < 0.05$ versus measurements before the start of the experiments by the Mann−Whitney *U* test. e.c., epicutaneous; OD, optical density.

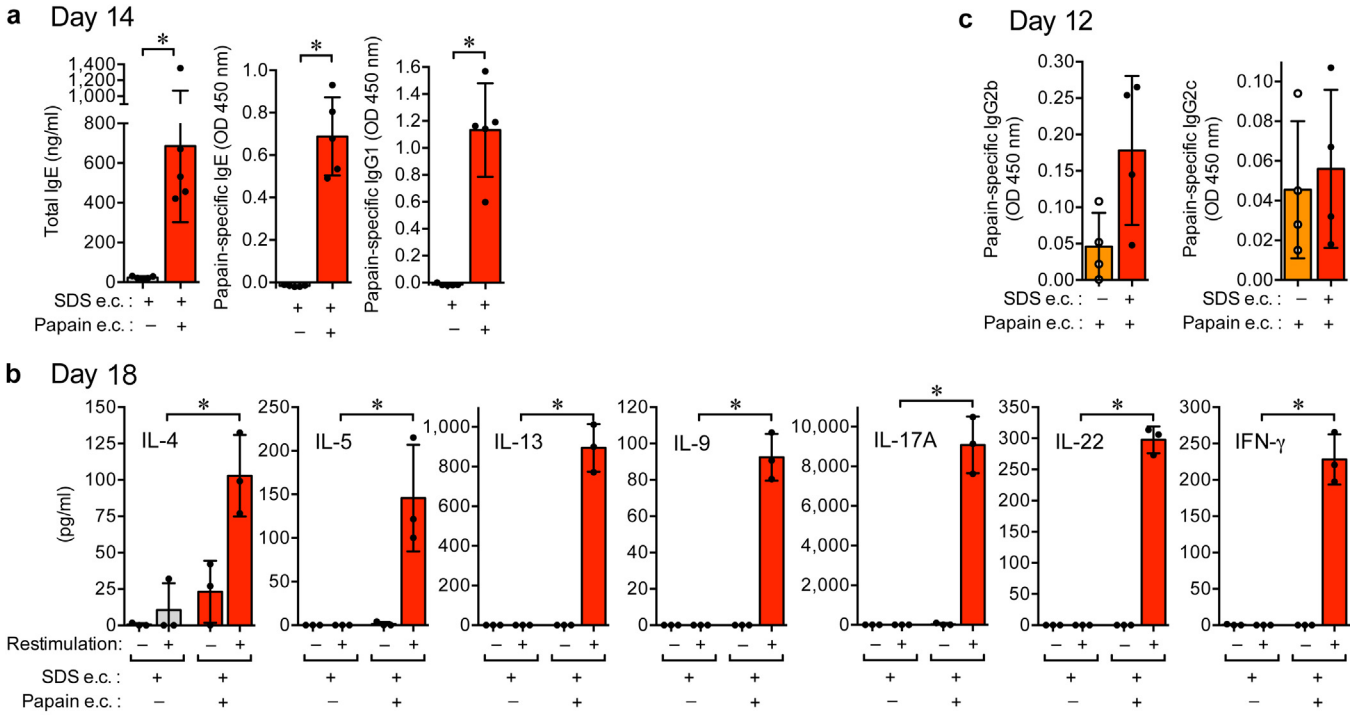

Supplementary Figure S2. Supplementary data for Figure 1. (**a, c**) Serum antibodies (n = 5 in **a**, and n = 4 in **b**). (**b**) Cytokine responses in skin DLN cells restimulated with E64-papain for 4 days (three wells). Data indicate means ± SD and are representative of two or more independent experiments. *$P < 0.05$ versus SDS e.c. + vehicle e.c. administration by the Mann−Whitney *U* test (for **a**) or *t*-test (for **b**). DLN, draining lymph node; e.c., epicutaneous; OD, optical density.

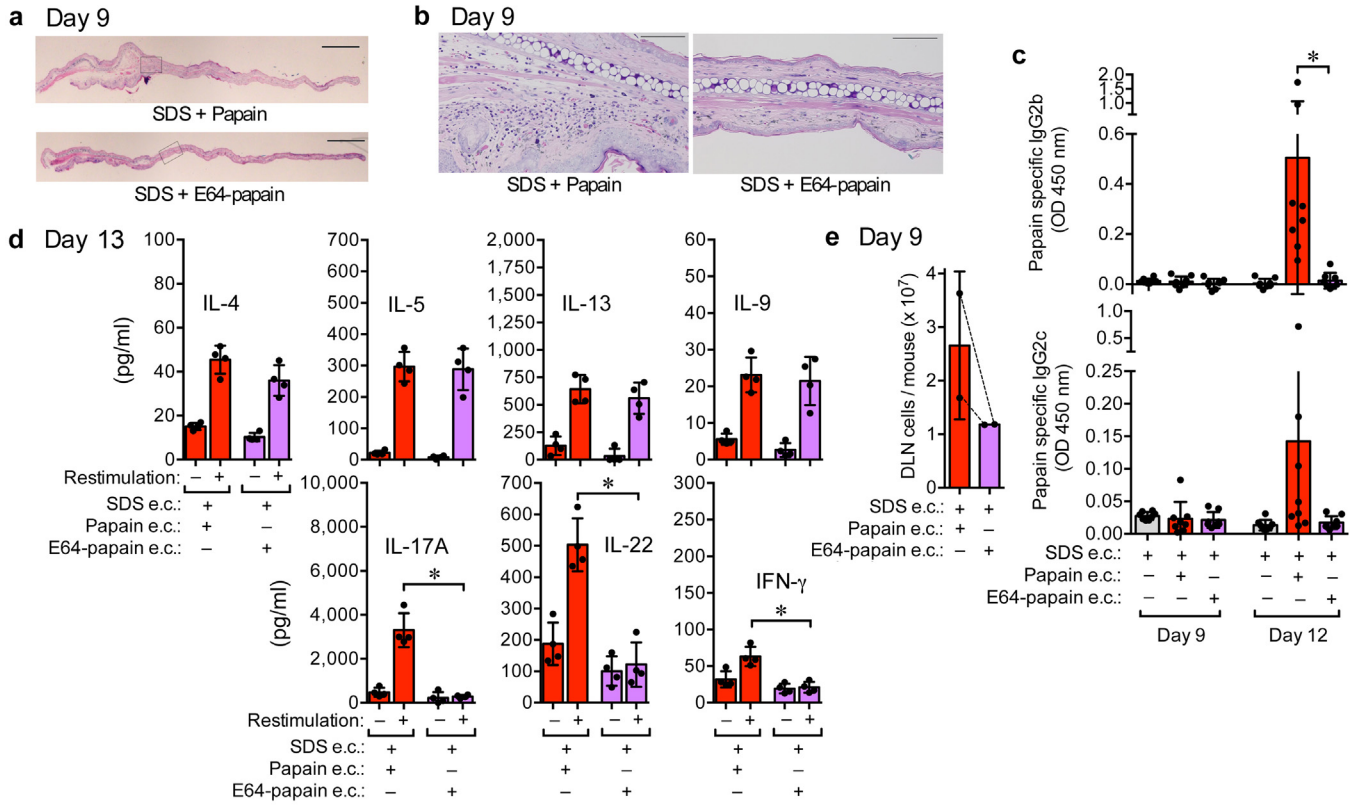

Supplementary Figure S3. Supplementary data for Figure 2a−i. (**a, b**) Histology (day 9). Bars = 1 mm (for **a**) and 0.1 mm (for **b**). (**c**) Serum papain−specific IgG2b and IgG2c (n = 8). (**d**) Cytokine responses in skin DLN cells, which were recovered on day 9 and were restimulated with E64-papain for 4 days (four wells). (**e**) Total cell numbers of DLN recovered on day 9. Data indicate means ± SD and are representative of two or more independent experiments. In **e**, each of the data points represents the averaged value in each of the independent experiments (n = 2), and the values for the papain epicutaneously treated and E64-papain epicutaneously treated groups obtained in the same independent experiments are linked with broken lines. *$P < 0.05$ by ANOVA. DLN, draining lymph node; e.c., epicutaneous; OD, optical density.

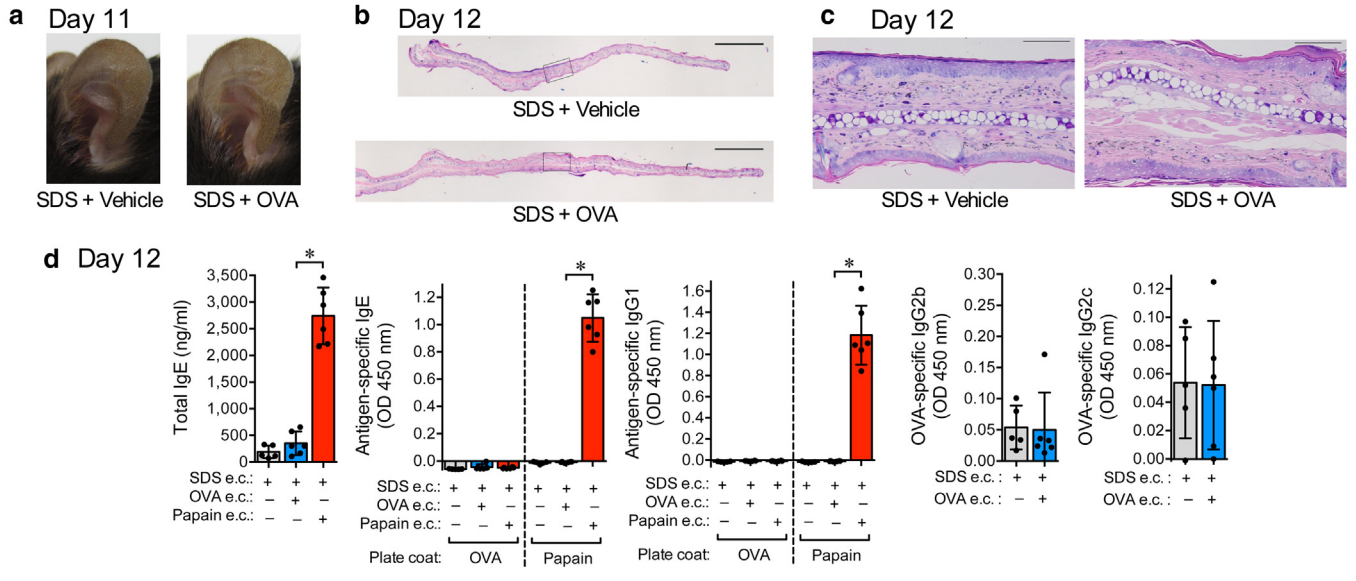

Supplementary Figure S4. Supplementary data for Figure 2j−l. (**a**) Appearance. (**b, c**) Histology. Bars = 1 mm (for **b**) and 0.1 mm (for **c**). (**d**) Serum antibodies (n = 5). Data indicate means ± SD and are representative of two or more independent experiments. *$P < 0.05$ versus OVA e.c. administration by ANOVA. e.c., epicutaneous; OD, optical density.